Deterministic diffusion generated by a chaotic map

Sona Prakash and Chung-Kang Peng
Center for Polymer Studies and Department of Physics, Boston University, Boston, Massachusetts 02215

Preben Alstrøm
Center for Polymer Studies and Department of Physics, Boston University, Boston, Massachusetts 02215
and Physics Laboratory, H.C. Øersted Institute, DK-2100 Copenhagen Ø, Denmark
(Received 28 June 1990; revised manuscript received 12 December 1990)

We describe one-dimensional discrete diffusive motion that is driven by a purely deterministic system, the logistic map. We find normal diffusive motion above a critical value λ_1^* of the chaotic parameter. At λ_1^*, the diffusion constant D plays the role of an order parameter, with a critical exponent of 1/2. In the presence of external noise, D is expressed in terms of a universal scaling function and the critical exponent associated with the noise is found to be 1. We also consider biased diffusive motion driven by the logistic map. We find that the diffusion process thus generated is different from random biased diffusion. In contrast to the case of the biased "random walker" where all configurations ("walks") are still possible, here certain configurations are not allowed. However, the statistical properties approach those for random biased diffusion in the infinite time limit. We define a measure of the effective randomness.

I. INTRODUCTION

Diffusion is normally associated with a stochastic driven force (a random variable). For Brownian motion,[1-3] the equation of motion is

$$M\ddot{x}+\gamma\dot{x}=\xi(t)\ , \tag{1}$$

where γ is the friction constant and M is the mass of the free particle. Equation (1) is also known as the Langevin equation, with the assumption that the $\xi(t)$ are Gaussian-correlated random forces (white noise):

$$\langle\xi(t)\rangle=0,\quad \langle\xi(t)\xi(t')\rangle\propto\delta(t-t')\ . \tag{2}$$

When the friction is high, i.e., $\gamma/M\gg 1$, the $\ddot{x}$ term can be neglected and (1) can be reduced to

$$\dot{x}(t)\propto\xi(t)\ , \tag{3}$$

and one obtains the normal diffusion law:[4]

$$\langle x(t)\rangle=0,\quad \langle x^2(t)\rangle\propto t\ . \tag{4}$$

In this paper, we consider the case where $\xi(t)$ is not random but deterministic and chaotic.[5,6] In Sec. II we set up a model for deterministic diffusion based on the logistic map $f(y)=4\lambda y(1-y)$,[7] and in Sec. III we discuss various properties of this map that are pertinent to this problem. We shall point out the similarities to the considerable amount of work done for circle-map diffusion.[8-12] We consider unbiased diffusion in Sec. IV and find normal diffusion for λ above a critical value λ_1^*, which is the first reverse bifurcation point for the map. We shall see that the diffusion constant plays the role of an order parameter at this point. The corresponding exponent is shown to be 1/2. In Sec. V we consider the effect of noise and derive the associated universal scaling properties. Finally, in Sec. VI we examine biased diffusion. This is found to differ from normal biased diffusion at small time scales, but approaches it in the infinite time limit with a given rate that depends on λ. We shall interpret this new exponent σ as a measure of how fast the system randomizes. We comment on the relation between σ and the Lyapunov exponent.

II. MODEL

For simplicity, we study one-dimensional discrete time nearest-neighbor lattice diffusion.[4] By choosing the time to be discrete, we are restricting ourselves in the time domain comparable to the time scale of molecular collisions. Thus $\xi(t)\to\xi(i)$, for $i=0,1,2,\ldots$. By nearest-neighbor lattice diffusion we mean that the particles can move only from one lattice site to a neighboring one, i.e., the particles move the same distance at each time step.

To generate the sequence of stochastic but deterministic driven forces, we use a chaotic map—the logistic map.[7] Consider

$$\xi(n)=\mathrm{sgn}(y_n-\phi)\ , \tag{5}$$

where the threshold ϕ can be regarded as controlling the external bias field. Thus, at time step n the particle will experience a rightward (leftward) force if y_n is greater (smaller) than ϕ and will take a step, $\xi(n)=+1(-1)$. In (5) y_n is generated by the logistic map, i.e.,

$$y_n=f_\lambda(y_{n-1})\equiv 4\lambda y_{n-1}(1-y_{n-1})\ , \tag{6}$$

with the initial value $y_0\in[0,1]$ randomly chosen for each particle. The trajectory of the particle is completely determined by the initial condition. In the following sections, the statistical properties of a system of particles that are governed by Eqs. (3), (5), and (6) will be studied by analytic methods as well as numerical simulations.

We shall only consider the chaotic regime of the logistic map, where $\lambda > \lambda_c \approx 0.8924$. We also restrict λ to be less than 1 to keep y_i in the unit interval.

In contrast to the diffusion studies for circle maps,[8-12] which add to the characterization of these maps in the chaotic regime, our study is motivated by the simplest random walk: A random number generator gives a number y between 0 and 1; then if $y<\phi$ the walker goes left, otherwise it goes right. In essence, what we are doing in Eqs. (5) and (6) is substituting the "external" random number generator by a chaotic map. Unlike the circle-map diffusion, the mechanism here allows us to incorporate easily symbolic dynamics into the problem; moreover, we are able to go easily from an unbiased random walk to a biased one by changing the value of the threshold ϕ. In particular, we can identify all walks as configurations of left and right steps and analyze the problem in terms of these configurations, both for the unbiased case (Sec. IV) and the biased case (Sec. VI). For example, we find that some configurations are excluded if the bias exceeds a certain value (Sec. VI).

III. LOGISTIC MAP

In this section we shall discuss the symbolic properties of the logistic map. Consider the logistic map (6) (Fig. 1), and a particle driven by this map. We are interested in spatial averages and start therefore from a uniform distribution of initial values y_0. Now, to find the statistical properties of our system we must know how often a particular sequence (which we call a *configuration)* of n steps (each step can be left or right, denoted by L or R, respectively) occurs. In order to answer this question we must calculate (i) in which interval $I(C)$ y_0 must be located to generate a particular configuration C, (ii) how often y_i will visit this interval. As regards (ii), we denote $P_\lambda(y)dy$ as the probability to find a particle between y and $y+dy$. Hence, the relative occurrence of a configuration C of length n is

$$\Gamma_n(C) \equiv \int_{I(C)} P_\lambda(y)dy \ . \tag{7}$$

To determine $I(C)$, consider a particle with value y_0. If we are interested in the first step of the particle (C of length 1) then we only need to compare y_0 with ϕ: if $y_0>\phi$, the particle steps to the right, if $y_0<\phi$ it steps to the left. Therefore $I(L)=(0,\phi)$ and $I(R)=(\phi,1)$ (Fig. 1). For the case of two time steps (C of length 2), we need also to compare $y_1=f_\lambda(y_0)$ with ϕ, or equivalently to find the inverse mapping of ϕ and compare it with y_0. In other words, if ϕ_1 and ϕ_2 are the inverse mappings of ϕ [i.e., $f_\lambda(\phi_1)=f_\lambda(\phi_2)=\phi$], and assume $\phi_2 \geq \phi_1$, then a particle with $y_0<\phi_1$ will take two steps to the left (C equals LL in Fig. 1) at the first two time steps, whereas y_0 in (ϕ_1,ϕ) will give rise to the LR configuration (if $\phi \leq \phi_2$), and so on. For the case of a three-step diffusion process we need to find the inverse iterates of ϕ_1, called ϕ_{11} and ϕ_{12} (choose $\phi_{11} \leq \phi_{12}$), and of ϕ_2, denoted by ϕ_{21} and ϕ_{22} ($\phi_{21} \leq \phi_{22}$). In general, for an n-step diffusion process, we need to trace back to the $(n-1)$th inverse iteration of ϕ, i.e., all the way to $\phi_{i_1 i_2 \cdots i_{n-1}}$ defined recursively by

$$f_\lambda(\phi_{i_1 \cdots i_m 1}) = f_\lambda(\phi_{i_1 \cdots i_m 2}) = \phi_{i_1 \cdots i_m}$$
$$(i_m=1,2, \quad m=1,\ldots,n-2) \ . \tag{8}$$

Analogously to the two time-steps case, $I(C)$ for a particular n-step configuration C has the form $(\phi_{i_1 \cdots i_m},$

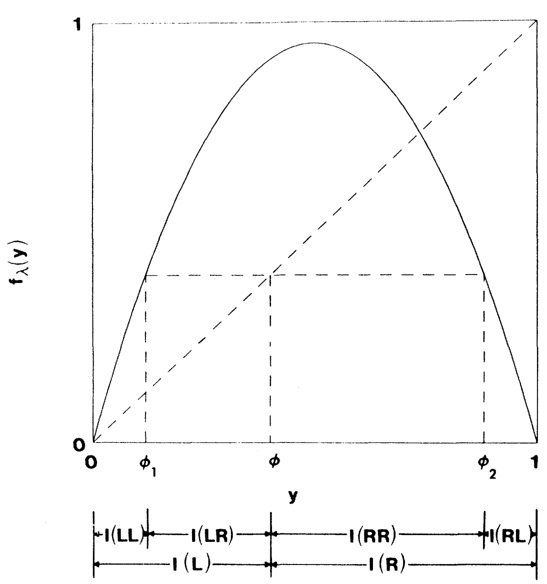

FIG. 1. The logistic map $f_\lambda(y)=4\lambda y(1-y)$.

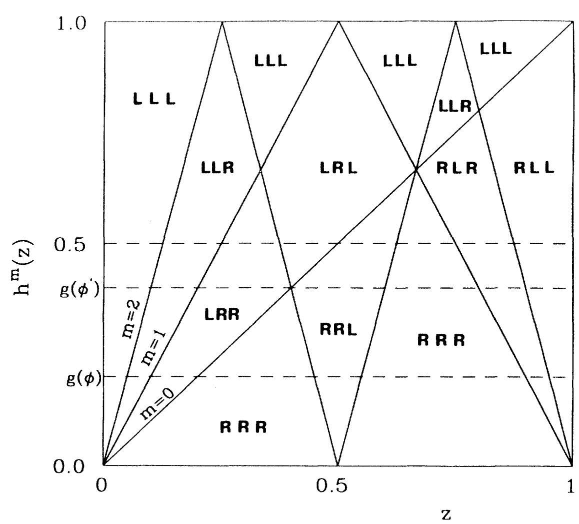

FIG. 2. All possible configurations at three time steps, for $\lambda=1$ found by iterating the tent map twice. At a given value of the bias field ϕ, the probability for a configuration C is given by the length of the intersection of the area corresponding to C with the line $h^m(z)=g(\phi)$. For $\phi=0.5$, $g(\phi)=0.5$ and all configurations are equally likely. Moreover, the probability for the configuration LRL is zero for $g(\phi) \leq g(\phi')=\frac{2}{5}$, on a log-log plot. The slope gives the diffusion constant for various values of λ.

$\phi_{i'_1 \cdots i'_k}$) with $m,k<n$.

For $\lambda=1$, the logistic map is equivalent to the tent map[13] (see Fig. 2 with $m=1$)

$$h(z)=\begin{cases}2z, & 0<z\le\frac{1}{2}\\ 2(1-z), & \frac{1}{2}<z\le 1\end{cases} \tag{9}$$

by a coordinate transformation $z=g(y)$ (see, e.g., Refs. 5 and 13). The probability density for $h(z)$ is uniform, so $P(y)=g'(y)$. Thus, for $I(C)=(\phi_{i_1\cdots i_m},\phi_{i'_1\cdots i'_k})$ we have

$$\Gamma_n(C)=g(\phi_{i'_1\cdots i'_k})-g(\phi_{i_1\cdots i_m}) . \tag{10}$$

Moreover, the relation $h^m(g(y))=g(f_1^m(y))$ identifies $g(\phi_{i_1\cdots i_m})$ as a solution to $h^m(z)=g(\phi)$. For $\lambda<1$, $P_\lambda(y)$ is not a smooth function and no simple analytic form for $\Gamma_n(C)$ exists.

IV. UNBIASED DIFFUSION

The threshold $\phi(\lambda)$ in (5) can be chosen such that the particles will experience the same amount of rightward and leftward forces (in a statistical sense). More precisely, we choose $\phi(\lambda)$ to have the value, denoted by $\phi_0(\lambda)$, that corresponds to $p=\Gamma_1(L)=\Gamma_1(R)=\frac{1}{2}$ where

$$\Gamma_1(L)\equiv\int_0^{\phi(\lambda)}P_\lambda(y)dy .$$

We call diffusion with this value of the threshold, *unbiased*, whereas the case $p\neq\frac{1}{2}$ is biased, and will be discussed in Sec. VI.

By definition, for unbiased diffusion,

$$\langle x(t)\rangle=0 . \tag{11}$$

For $\lambda=1$, we have $\phi_0(1)=\frac{1}{2}$ since then $\Gamma_1(L)=g(\frac{1}{2})=\frac{1}{2}$. To find the probability of occurrence $\Gamma_n(C)$ of a particular configuration of length n, we need to determine the corresponding interval $I(C)$. The end points of the intervals are given by the solutions to $h^m(z)=\frac{1}{2}$ $(0\le m\le n-1)$. These solutions are $k/2^n$ $(k=1,2,\ldots,2^n-1)$ [in Fig. 2, intervals marked by intersections with the line $h^m(z)=\frac{1}{2}$ are all of the same length]. From (10) we have

$$\Gamma_n(C)=(\tfrac{1}{2})^n \tag{12}$$

for all C of length n. This is exactly the same as for unbiased random walks, which means that one cannot see the deterministic effect in the statistical quantities we measure. As a concrete example, the diffusion law does not change, i.e.,

$$\langle x^2(t)\rangle=t \quad (\lambda=1) , \tag{13a}$$

the same as the result for unbiased random walks.

For $\lambda<1$ only numerical studies have been done. By carefully choosing ϕ to make the first moment of the displacement vanish, i.e., $\langle x(t)\rangle=0$, we found the unbiased threshold $\phi_0(\lambda)$. From the numerical data we find that the diffusion behavior of the particles is still *normal*,

$$\langle x^2(t)\rangle=D(\lambda)t , \tag{13b}$$

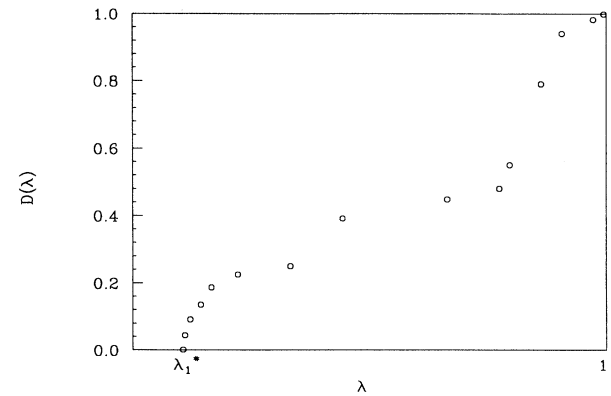

FIG. 3. Diffusion constant $D(\lambda)$.

where $D(\lambda)$ is the diffusion constant which, however, depends on λ. D has the value 1 at $\lambda=1$. As we decrease the value of λ, D also decreases (Fig. 3); in particular, D vanishes at the first reverse bifurcation point[5] $\lambda=\lambda_1^*\approx 0.919\,64$ (Fig. 4).

The reason why $D=0$ for $\lambda\le\lambda_1^*$ is clear in view of the bifurcation diagram (Fig. 4): After a transient period, the numbers generated from the logistic map for $\lambda\le\lambda_1^*$ oscillate between two chaotic intervals that are located on the two opposite sides of $\phi_0(\lambda)$ (the unbiased threshold). This means that a particle will always experience a rightward (leftward) force after a leftward (rightward) force, i.e., the particles will oscillate and never move away.[14]

For λ slightly larger than λ_1^*, this alternating behavior is perturbed but it still exists within a characteristic time scale $\tau^*(\lambda)$. Figure 5 shows a typical particle trajectory. Within a certain time scale $t<\tau^*(\lambda)$ the particle oscil-

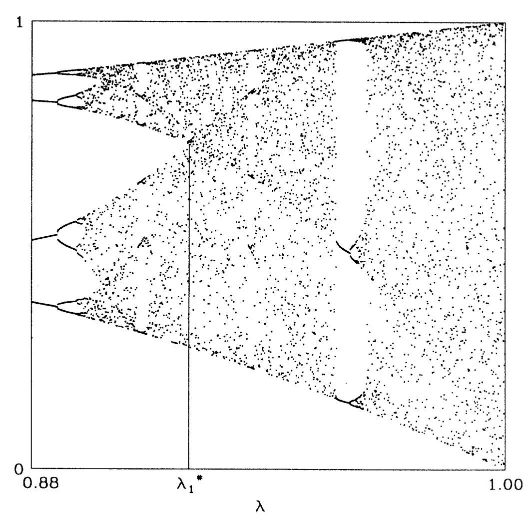

FIG. 4. Bifurcation diagram for the logistic map (6000 data points): Notice the window the appears below $\lambda=\lambda_1^*$, dividing the phase space into two chaotic intervals for $\lambda\le\lambda_1^*$.

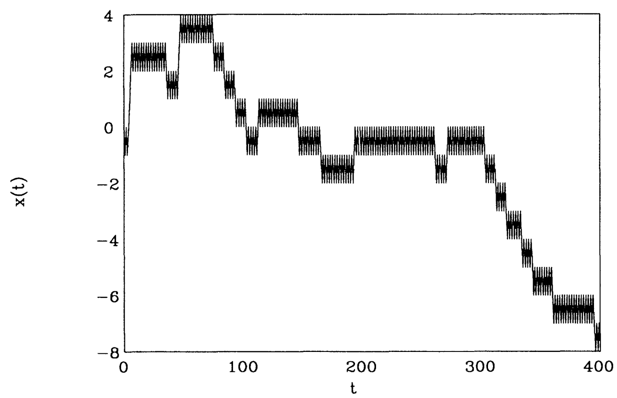

FIG. 5. A typical particle trajectory for $\lambda=0.925$.

lates around some fixed point, while for $t>\tau^*(\lambda)$ the particle seems to behave like a random walker. This suggests the following conjecture:

$$D(\lambda)\sim\frac{1}{\tau^*(\lambda)} . \tag{14}$$

In this respect D can be thought of as an order parameter.

As we approach $\lambda=\lambda_1^*$ from above, this characteristic time $\tau^*(\lambda)$ diverges. We are interested in seeing how τ^* scales with $\delta\lambda=\lambda-\lambda_1^*$ for small $\delta\lambda$. At $\lambda=\lambda_1^*$, the unbiased threshold $\phi_0(\lambda)$ is the same as the unstable fixed point $\alpha(\lambda)=1-1/4\lambda$. The point $\lambda=\lambda_1^*$ is characterized by $f_{\lambda_1^*}(\lambda_1^*)=1/4\lambda_1^*$ or

$$f^3_{\lambda_1^*}(\tfrac{1}{2})=\alpha(\lambda_1^*) . \tag{15}$$

The interval $A=(1/4\lambda_1^*,\alpha(\lambda_1^*))$ maps into the interval $B=(\alpha(\lambda_1^*),\lambda_1^*)$ and vice versa $A\overset{f}{\leftrightarrow}B$ [Fig. 6(a)]. Now, consider $\lambda=\lambda_1^*+\delta\lambda$ for small $\delta\lambda$. Then (15) is modified to

$$f^3_\lambda(\tfrac{1}{2}\pm\delta y)=\alpha(\lambda) . \tag{16}$$

There is now a finite probability for the trajectory to deviate from oscillatory behavior. From Fig. 6(b) it can be seen that this happens when the trajectory hits a value in the interval $I(\delta y)\equiv(\frac{1}{2}-\delta y,\frac{1}{2}+\delta y)$. Until we "hit" a

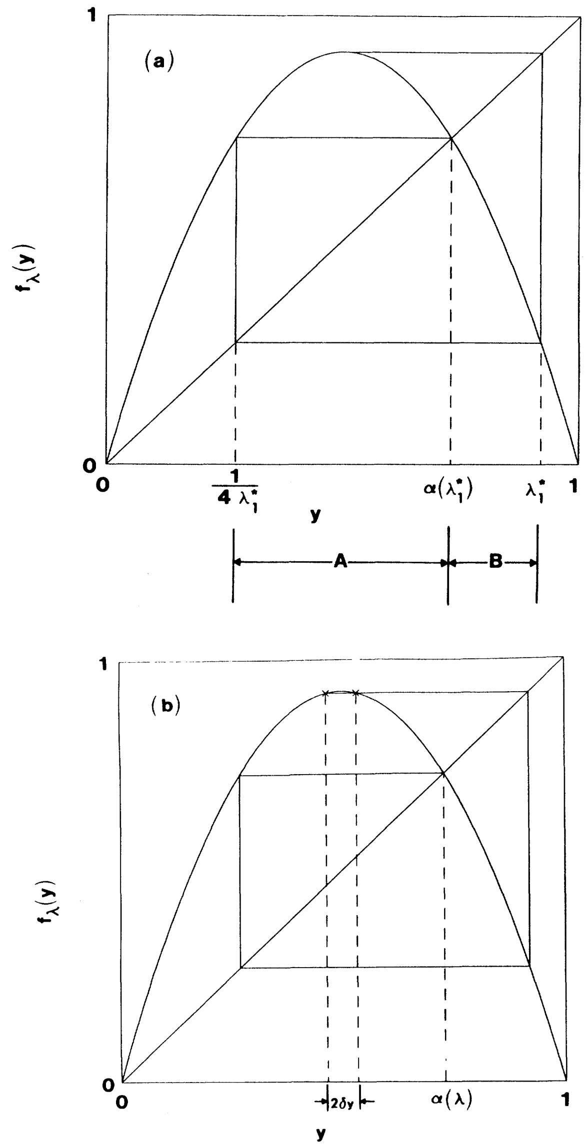

FIG. 6. (a) $\lambda=\lambda_1^*$; the point $y=\frac{1}{2}$ maps in three iterations into the unstable fixed point $\alpha(\lambda_1^*)=1-1/4\lambda_1^*$. (b) $\lambda=\lambda_1^*+\delta\lambda$; the points that map into the unstable fixed point $\alpha(\lambda)$ in three iterations are given by $\frac{1}{2}\pm\delta y$.

number in this interval, the trajectory continues to go alternately above and below the unbiased threshold, which is now slightly below the unstable fixed point $\alpha(\lambda)$. Thus the diffusive motion of the particle originates from the interval $I(\delta y)$. We can find the dependence of δy on $\delta\lambda$ by Taylor expansion of $f^3_\lambda(y)$ at $y=\frac{1}{2}$ and $\lambda=\lambda_1^*$:

$$f^3_\lambda(y)=f^3_{\lambda_1^*}(\tfrac{1}{2})+\left.\frac{d^2f^3_{\lambda_1^*}}{dy^2}\right|_{y=1/2}\frac{(\delta y)^2}{2}+\left.\frac{df^3_\lambda(\frac{1}{2})}{d\lambda}\right|_{\lambda=\lambda_1^*}\delta\lambda+\cdots \tag{17}$$

$(df^3_{\lambda_1^*}/dy|_{y=1/2}=0)$. This gives to leading order in δy and $\delta\lambda$

$$\delta y \sim (\delta\lambda)^{1/2} . \tag{18}$$

Next, we relate δy to τ^*, the characteristic time scale. To this end, we notice that τ^* is the average first return time for particles in $I(\delta y)$. We write

$$\tau^* = \tau_f + \tau_h , \tag{19}$$

where τ_f is the time it takes the trajectory to "forget" that it originated from $I(\delta y)$, and τ_h is the average time it then takes to get to $I(\delta y)$ again. To find τ_f we start N particles in $I(\delta y)$ distributed homogeneously on the attractor (with $\lambda=\lambda_1^*+\delta\lambda$). As argued above [see (16) and (18)], after three iterations the particles will be located in an interval of size $(\delta y)^2$ at $\alpha(\lambda_1^*)$. This interval will then expand in size by a factor of $\Lambda=|f'_{\lambda_1^*}(\alpha(\lambda_1^*))|$ at each following iteration ($\Lambda\simeq 1.68$). The information that the particles originated from $I(\delta y)$ is therefore lost at time τ_f given by

$$\Lambda^{\tau_f}(\delta y)^2 \sim 1 , \tag{20}$$

hence

$$\tau_f \sim |\ln\delta y| . \tag{21}$$

At time τ_f the particles are effectively scattered homogeneously over the entire attractor. We shall assume that $N(\tau_f)=2\delta y N$ of them will be located in $I(\delta y)$. Moreover, since the Lyapunov exponent at $\lambda=\lambda_1^*$ is of order 1, we can assume that the rest $(1-2\delta y)N$ of the particles at time τ_f+1 are again distributed homogeneously on the attractor. Hence, $N(\tau_f+1)=(1-2\delta y)2\delta y N$ will hit $I(\delta y)$ at time τ_f+1. At time τ_f+2, $N(\tau_f+2)=(1-2\delta y)^2\, 2\delta y N$ will hit $I(\delta y)$, and so on. In general, $N(\tau_f+\tau)=(1-2\delta y)^\tau 2\delta y N$ will hit $I(\delta y)$ at time $\tau_f+\tau$. The average time τ_h is

$$\tau_h = \frac{1}{N}\sum_{\tau=0}^{\infty} \tau N(\tau_f+\tau) = (1-2\delta y)/\delta y \sim (\delta y)^{-1} . \tag{22}$$

For small δy, $\tau_h \gg \tau_f$, and $\tau^* \simeq \tau_h$. From (18) and (22) we have[15]

$$\tau^*(\lambda) \sim (\delta\lambda)^{-1/2} . \tag{23}$$

We also calculated the diffusion constant directly from numerical data for the scaling of the second moment with time near $\lambda=\lambda_1^*$ (Fig. 7). The result agrees with the λ dependence derived from (14) and (23),

$$D(\lambda) \sim (\lambda-\lambda_1^*)^{1/2} . \tag{24}$$

At $\delta\lambda \simeq 10^{-3}$, $\tau_f \sim \tau_h$, and corrections to (24) become important. The same scaling behavior for the diffusion constant with the nonlinearity parameter has been obtained in a circle-map system[8] where diffusion is generated by a different mechanism—the value 1/2 of the exponent in Eq. (24) is merely a consequence of the fact that the map has a quadratic maximum; for a maximum of order z, the exponent is[8] $1/z$ [in Eq. (17), the first $z-1$ derivatives of $f^3_\lambda(y)$ at $y=\frac{1}{2}$ will be zero, thus $\delta y \sim (\delta\lambda)^{1/z}$].

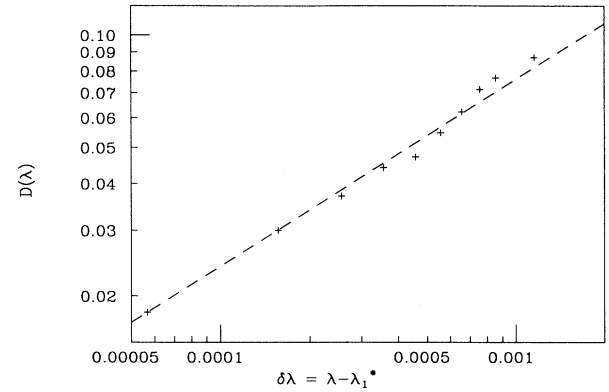

FIG. 7. Results of numerical simulations on logarithmic scale showing $D(\lambda)\sim(\lambda-\lambda_1^*)^{1/2}$.

To elaborate on the result (23), consider the autocorrelation function $C(m)$ defined by

$$C(m)=\langle \xi(i)\xi(i+m)\rangle = \lim_{N\to\infty}\frac{1}{N}\sum_{i=0}^{N-1}\xi(i)\xi(i+m) , \tag{25}$$

where $\xi(i)$ is given by (5) with $y_i=f^i_\lambda(y_0)$. For λ slightly above λ_1^*, we find numerically that $C(m)$ decays exponentially,

$$|C(m)| \sim \exp\left[-\frac{m}{\tau_c(\lambda)}\right] . \tag{26}$$

Here $\tau_c(\lambda)$ is the characteristic time over which correlations exist. We expect that $\tau_c(\lambda)\sim\tau^*(\lambda)$, i.e., from (19),

$$\tau_c(\lambda) \sim (\lambda-\lambda_1^*)^{-1/2} . \tag{27}$$

Numerical studies confirm this relation. Again we find corrections to scaling when τ_f and τ_h are of the same order.

V. UNBIASED DIFFUSION WITH NOISE

In this section we will discuss unbiased deterministic diffusion with "external noise." We add noise to the system in the following way: instead of completely following the trajectory that is determined by the sequence of chaotic numbers, the particle can disobey the rule and move in the opposite direction with a certain probability ϵ, the magnitude of the external noise. If $\xi'(i)$ denotes the displacement of the particle at time i with noise,

$$\xi'(i)=\begin{cases}-\xi(i) & \text{with probability } \epsilon,\\ \xi(i) & \text{with probability } 1-\epsilon .\end{cases} \tag{28a}$$

The autocorrelation function $C(m)$ is modified,

$$\begin{aligned}\langle \xi'(i)\xi'(j)\rangle &= [(1-\epsilon)^2+\epsilon^2-2\epsilon(1-\epsilon)]\langle\xi(i)\xi(j)\rangle\\ &= [1-4\epsilon(1-\epsilon)]\langle\xi(i)\xi(j)\rangle \quad \text{for } i\neq j ,\end{aligned} \tag{28b}$$

and

$$\langle \xi'(i)\xi'(j)\rangle = \langle \xi(i)\xi(j)\rangle \quad \text{for } i=j\ . \tag{28c}$$

For $\lambda \le \lambda_1^*$, the particle will oscillate forever if there is no noise, thus

$$\langle \xi(i)\xi(j)\rangle = \begin{cases} 1 & \text{if } |i-j| \text{ is even,} \\ -1 & \text{if } |i-j| \text{ is odd}\ . \end{cases} \tag{29}$$

From (28) the diffusion coefficient $D(\epsilon,\lambda \le \lambda_1^*)$ can be calculated,

$$\begin{aligned} \langle x^2(t)\rangle &= \left\langle \left[\sum_{i=1}^{t} \xi'(i) \right]^2 \right\rangle \\ &= \sum_{i=1}^{t} \sum_{j=1}^{t} \langle \xi'(i)\xi'(j)\rangle \\ &= \sum_{i=1}^{t} \langle \xi'^2(i)\rangle + \sum_{\substack{j,k=1 \\ j\neq k}}^{t} \langle \xi'(j)\xi'(k)\rangle \\ &\approx t - [1-4\epsilon(1-\epsilon)]t = 4\epsilon(1-\epsilon)t\ . \end{aligned} \tag{30}$$

Thus, $D(\epsilon,\lambda \le \lambda_1^*) = 4\epsilon(1-\epsilon)$. In particular,

$$D(\epsilon,\delta\lambda \to 0) \sim \epsilon \tag{31a}$$

for small ϵ. From (24), we have

$$D(\epsilon \to 0,\delta\lambda) \sim (\delta\lambda)^{1/2} \tag{31b}$$

for small $\delta\lambda$. The scaling relations (31a) and (31b) suggest the following scaling form for $D(\epsilon,\delta\lambda)$:

$$D(\epsilon,\delta\lambda) = \epsilon G\left[\frac{\delta\lambda}{\epsilon^2}\right] \tag{32}$$

($\delta\lambda$ and ϵ small),[16] with

$$G(x) \sim \begin{cases} \text{const} & \text{as } x \to 0, \\ x^{1/2} & \text{as } x \to \infty\ . \end{cases} \tag{33}$$

We have verified this relation numerically (Fig. 8).

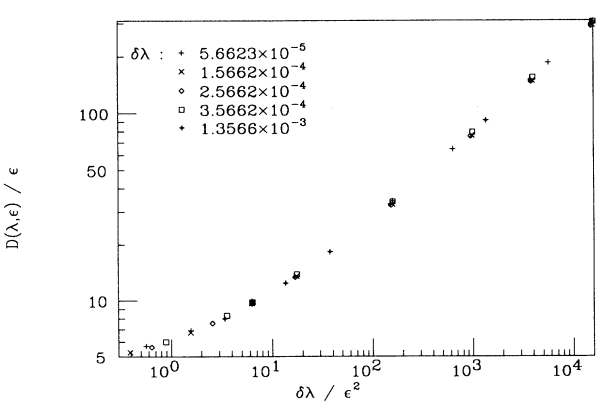

FIG. 8. Universal scaling behavior of the diffusion constant D.

VI. BIASED DIFFUSION

If the threshold ϕ in (5) in chosen in such a way that the rightward and leftward forces are not the same, the process is called biased diffusion. In this case we have

$$\langle x(t)\rangle = (p-q)t\ , \tag{34}$$

where $p=\Gamma_1(L)$ and $q=\Gamma_1(R)=1-p$. We call p the *bias*. As discussed at the beginning of Sec. IV, biased diffusion corresponds to $p\neq\frac{1}{2}$ and $\phi\neq\phi_0(\lambda)$. Thus, here we fix $\phi(\lambda)$ at some value away from the unbiased threshold $\phi_0(\lambda)$.

In contrast to random diffusion, at each time step, the probabilities to go left or right do not split in the ratio of $p:q$. This is also the case for $\lambda=1$. For example, for $\phi=0.4$ we have $p=g(\phi)\simeq 0.436$ and $q\simeq 0.564$. For the second time step,

$$\Gamma_2(LL)\simeq 0.218 > p^2\ ,$$

$$\Gamma_2(LR)\simeq 0.218 < pq\ ,$$

$$\Gamma_2(RR)\simeq 0.346 > q^2\ ,$$

$$\Gamma_2(RL)\simeq 0.218 < pq\ .$$

In general, there is no simple expression for $\Gamma_n(C)$, unlike the unbiased case [cf. (12)].

The probability for going left or right at each time step depends on the previous history of the system and thus one needs to calculate Γ_m for all previous time steps $m<n$ in order to obtain $\Gamma_n(C)$. Moreover, there are certain configurations that do not exist. To illustrate this topological constraint consider $\lambda=1$. Using the tent-map analog (Sec. IV), the probabilities of occurrence $\Gamma_n(C)$ of existing configurations C of length n are found from the end points of the intervals $I(C)$, which are given by solutions to $h^m(z)=g(\phi)$ $(0\le m\le n-1)$. As shown in Fig. 2, the configuration LRL does not exist below $g(\phi')=\frac{2}{5}$ $(\phi<\phi'\simeq 0.36)$, it is said to be *pruned*.[17] In general, we can write for an n-step diffusion process

$$\langle x^2(n)\rangle = \sum_C \Gamma_n(C)(n-2n_L)^2\ , \tag{35}$$

where n_L is the number of steps taken to the left. Since $I(C)$ is an interval between two pre-images $\phi_{i_1\cdots i_m}$ and $\phi_{i_1'\cdots i_k'}$ $(k\le m<n)$ (cf. Sec. III), the value of $\Gamma_n(C)$ is well approximated by $[(f^m)'(\phi_{i_1\cdots i_m})]^{-1}$ for large n.

For a random diffusion process with a bias,[4]

$$\langle x^2(t)\rangle = (p-q)^2t^2 + 4pqt\ . \tag{36}$$

For the $\lambda=1$ chaotic process we have calculated exactly the values of $\langle x^2(t)\rangle$ for small times t from the $\Gamma_t(C)$ and found that they deviated from the expression (36). Moreover, the values of $\langle x^2(t)\rangle$ are different for two values of the bias (corresponding to two values of the threshold, say, ϕ and ϕ^*) that are equidistant from the unbiased point $p=\frac{1}{2}$ (corresponding to ϕ_0) and on either side of it (i.e., favoring rightward or leftward forces, respectively, by the same amount). This is completely different from a random biased diffusion process. In Fig.

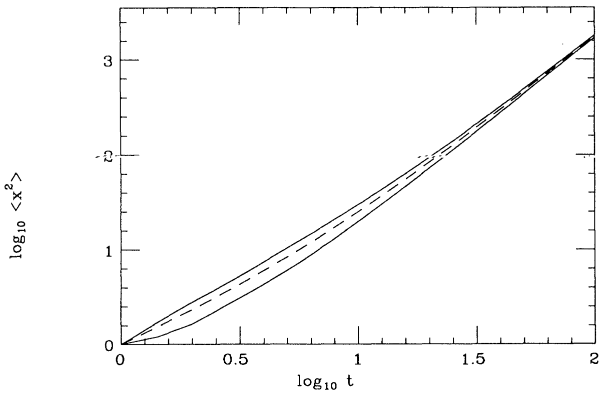

FIG. 9. Biased diffusion shows deviation from random biased diffusion (dotted curve). The upper and lower bold curves represent $\phi=0.2$, $\phi^*=0.8$, respectively.

9 we have plotted $\log_{10}\langle x^2(t)\rangle$ versus $\log_{10}t$ for $\lambda=1$ ($\phi=0.2$, $\phi^*=0.8$). We observe that the curves for ϕ and ϕ^* lie on either side of the curve (36) for the random process and that they approach the curve for the random process at large times. The chaotic biased diffusion process becomes like the random one at large times.

We are interested in the rate at which the random process is approached as we increase the number of iterations of the logistic map, i.e., the number of time steps. For this purpose we do as follows: Instead of taking every successive number generated by the map, we take every mth number. We denote the probability of a configuration C after n time steps by $\Gamma_n^m(C)$. For example,

$$\Gamma_2^4(LL)=\sum_X \Gamma_5^1(LXL) , \tag{37}$$

where the sum is over all three-step configurations X, and $\Gamma_n^1(C)=\Gamma_n(C)$. For random biased diffusion,

$$\Gamma_n(C,\phi)=\Gamma_n(C^*,\phi^*) , \tag{38}$$

where the configuration C^* corresponds to the reverse $(R,L\to L,R)$ of C. Based on this observation, we define a measure of the *effective randomness* of the process as

$$\Delta_m=|\Gamma_2^m(LL,\phi)-\Gamma_2^m(RR,\phi^*)| . \tag{39}$$

We find that Δ_m decays exponentially,

$$\Delta_m \sim \exp(-m\sigma) , \tag{40}$$

with a rate σ that depends on λ.

For $\lambda=1$, σ can be determined analytically using the tent-map transformation. To obtain $\Gamma_2^m(LL,\phi)$ and $\Gamma_2^m(RR,\phi^*)$ we consider $h^m(z)$ (Fig. 10). $\Gamma_2^m(LL,\phi)$ is the length of the intersection of $g(\phi)$ with the area in Fig. 10 *above* z and $h^m(z)$, while $\Gamma_2^m(RR,\phi^*)$ is the length of the intersection of $g(\phi^*)=1-g(\phi)$ with the area *below* z and $h^m(z)$. This intersection is shown with bold lines in Fig. 10. Each *complete* bold line has length $g(\phi)/2^{m-1}$ and there are approximately $2^{m-1}g(\phi)$ of them, giving a length $[g(\phi)]^2$ plus an additional part of length

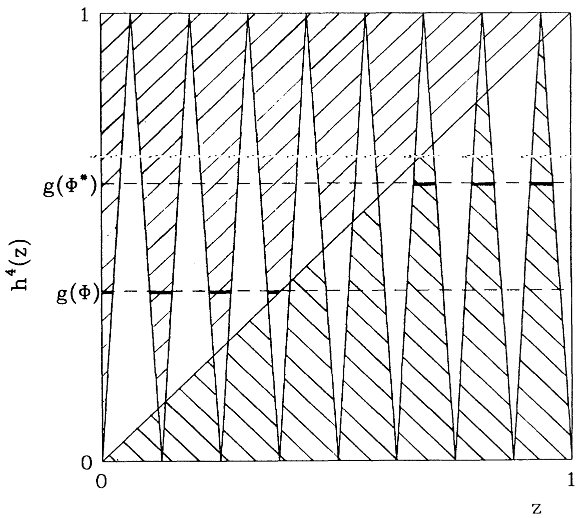

FIG. 10. Fourth iteration of the tent map $[g(\phi^*)=1-g(\phi)]$. Lower and upper set of bold lines indicate portion that contributes to $\Gamma_2^5(\mathrm{LL},\phi)$ and $\Gamma_2^5(\mathrm{RR},\phi^*)$, respectively.

$g(\phi)F_m(g(\phi))/2^{m-1}$ where $-\frac{1}{2}\le F_m(z)\le\frac{1}{2}$. From this geometrical picture, we easily obtain

$$\Gamma_2^m(LL,\phi)\simeq\Gamma_2^m(RR,\phi^*)\simeq[g(\phi)]^2=p^2 , \tag{41}$$

with correction

$$\Delta_m=2g(\phi)\frac{F_m(g(\phi))}{2^m} , \tag{42a}$$

or

$$\Delta_m=2g(\phi)F_m(g(\phi))\exp(-m\ln 2) . \tag{42b}$$

Thus, $\sigma(\lambda=1)=\ln 2$. This agrees with our numerical results: in Fig. 11 we have plotted $\ln\Delta_m$ versus m. We find that Δ_m does not decrease monotonically with m, but displays steplike behavior. This can be attributed to the variation in the function F_m with m, which is related to the pruning of certain configurations at certain numbers

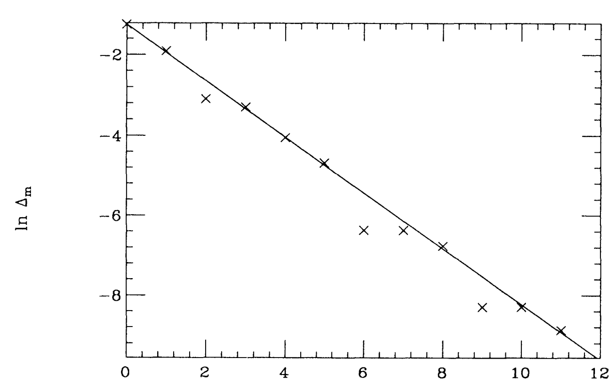

FIG. 11. Plot of $\ln\Delta_m$ vs m for $\lambda=1$; $\phi,\phi^*=0.2,0.8$. The straight line has slope $\sigma=-\ln 2$.

m of time steps. The envelope of the steps is, however, a straight line (shown in Fig. 11) with slope $= -\ln 2$. We notice that the value of the Lyapunov exponent at $\lambda = 1$ is ln2 as well. We speculate that $\sigma(\lambda)$ also equals the Lyapunov exponent below $\lambda = 1$, but we have not been able to obtain a clear indication due to fluctuation in Δ_m. For $\lambda \leq \lambda_1^*$, $\Delta_m = 0$, and σ is not defined.

VII. SUMMARY

In this paper we have set up a general formalism for describing the diffusion properties of a deterministic walk generated by an "external" chaotic map. The formalism is easily applied to the case of an arbitrary bias field (as we have shown in Sec. VI) and also incorporates symbolic dynamics. The latter enables us to make a connection with the formalism of Ref. 17. We have first described the unbiased diffusion for the logistic map in the chaotic regime, and identified the diffusion constant D as an order parameter at λ_1^*, characterizing a transition from a "localized" regime below λ_1^* in which the particle just oscillates about one point and does not diffuse at all, to a regime with normal diffusion. We have derived the value of the order parameter exponent, both analytically and numerically, and have found it to have a value of 1/2. The same scaling behavior was obtained in Ref. 8 for a different diffusive mechanism and thus a different transition point. The short-range correlations (exponential decay) of the logistic map near λ_1^* is related to the value of D. We have also considered the effect of noise on the diffusion constant and derived the resulting universal scaling properties. A similar scaling behavior for D is obtained for the diffusive motion in circle maps.

Second, we have extended the model to the case of biased diffusion and studied its properties in the same regime of the map, and have found them to differ from those of the corresponding random process but to approach these in the infinite time limit, with a rate that depends on the chaotic parameter λ. This rate σ is derived to be equal to the Lyapunov exponent for $\lambda = 1$ and we speculate that this is true for lower values of λ above λ_1^* as well. However, for $\lambda \leq \lambda_1^*$, σ is not defined. In addition, we find that biased diffusion results in the pruning of certain configurations.

ACKNOWLEDGMENTS

We would like to thank H. J. Herrmann and H. E. Stanley for enlightening conversations that initiated this work,[18] S. Havlin for motivating us to study the effect of noise on unbiased diffusion, and D. Stauffer and H. Larralde for useful discussions. The Center for Polymer Studies is supported by grants from the National Science Foundation, the Office of Naval Research, and British Petroleum. One of us (P.A.) also acknowledges support from the Danish Natural Science Research Council and the Carlsberg Foundation.

[1] M. C. Wang and G. E. Uhlenbeck, Rev. Mod. Phys. **17**, 323 (1945).

[2] N. G. van Kampen, *Stochastic Processes in Physics and Chemistry* (North-Holland, Amsterdam, 1981).

[3] E. W. Montroll and B. J. West, *Fluctuation Phenomena* (North-Holland, Amsterdam, 1979).

[4] See, e.g., S. Chandrasekhar, Rev. Mod. Phys. **15**, 1 (1943).

[5] See, e.g., H. G. Schuster, *Deterministic Chaos* (Physik-Verlag, Weinheim, 1988).

[6] T. Shimizu, Physica A **164**, 123 (1990).

[7] See, e.g., M. J. Feigenbaum, Los Alamos Sci. **1**, 4 (1980).

[8] T. Geisel and J. Nierwetberg, Phys. Rev. Lett. **48**, 7 (1982).

[9] M. Schell, S. Fraser, and R. Kapral, Phys. Rev. A **26**, 504 (1982).

[10] S. Grossmann and H. Fujisaka, Phys. Rev. A **26**, 1779 (1982).

[11] H. Fujisaka and S. Grossmann, Z. Phys. B **48**, 261 (1982).

[12] S. Grossmann and S. Thomae, Phys. Lett. A **97**, 263 (1983).

[13] See, e.g., A. J. Lichtenberg and M. A. Lieberman, *Regular and Stochastic Motion* (Springer-Verlag, Berlin, 1983).

[14] Of course, the logistic map itself still shows diffusion properties below λ_1^*; this has been studied [S. Grossmann and S. Thomae, Z. Naturforsch. A **32**, 1353 (1977)] by considering f^2 instead of f, thus restricting the trajectory to one of the two chaotic intervals and then considering f^4 and so on at each successive reverse bifurcation point. To study the corresponding diffusion problem we would then have to replace f_λ by $f_\lambda^{2^n}$ (at the nth reverse bifurcation point) in (6) and substitute this in (5), along with a corresponding suitably redefined ϕ. However, in this paper we are interested in the properties of a deterministic walker whose dynamics is defined by the particular sign function (5) composed by the logistic map, and this shows no diffusion below λ_1^*.

[15] The analysis leading to this result is similar to the analysis of the intermittency route to chaos near a periodic window [J. E. Hirsch, B. A. Huberman, and B. J. Scalapino, Phys. Rev. A **25**, 519 (1983)].

[16] The exponent of the noise is different from the exponent derived in Ref. 8, because the natural way of defining the noise and its amplitude is different. For the effect of noise on maps, see, e.g., J. P. Crutchfield, J. D. Farmer, and A. B. Hubermann, Phys. Rep. **92**, 45 (1982).

[17] P. Cvitanović, Phys. Rev. Lett. **61**, 2729 (1988).

[18] C. K. Peng, S. Prakash, H. J. Herrmann, and H. E. Stanley, Phys. Rev. A **42**, 4537 (1990).